Higher Order Response in $\mathcal{O}(N)$ by Perturbed Projection

Valéry Weber[†]
Department of Chemistry, University of Fribourg, 1700 Fribourg, Switzerland.
Anders M. N. Niklasson and Matt Challacombe
Los Alamos National Laboratory, Theoretical Division,
Los Alamos 87545, New Mexico, USA.

(Dated: December 21, 2004)

Abstract

Perturbed projection for linear scaling solution of the coupled-perturbed self-consistent-field equations [Weber, Niklasson and Challacombe, Phys. Rev. Lett. **92**, 193002 (2004)] is extended to the computation of higher order static response properties. Although generally applicable, perturbed projection is developed here in the context of the self-consistent first and second electric hyperpolarizabilities of three dimensional water clusters at the Hartree-Fock level of theory. Non-orthogonal, density matrix analogues of Wigner's $2n+1$ rule are given up to fourth order. Linear scaling and locality of the higher order response densities under perturbation by a global electric field are demonstrated.

PACS numbers: 02.70.-c, 71.15.Dx,31.15.Ar,31.15.Md,31.15.Ne,33.15.Kr,36.40.Cg

I. INTRODUCTION

First principles electronic structure theory has traditionally been limited to the study of small systems with a limited number of nonequivalent atoms. Despite the tremendous increase in computational power of digital computers this has remained the case, until the advent of reduced complexity algorithms over the last decade [1–6]. In the best case, these reduced complexity algorithms scale only linearly with system size, N, allowing simulation capabilities to keep pace with hardware improvements. These linear scaling algorithms exploit the quantum locality (or nearsightedness) of non-metallic systems, manifested in the approximate exponential decay of density matrix elements with atom-atom separation through the effective use of sparse matrix methods. For small systems, linear scaling methods may be inefficient due to overhead. However, for large, complex systems these methods hold the promise of major impact across materials science, chemistry and biology.

So far, a majority of work in linear scaling electronic structure theory has focused on methods and calculations involving the ground state, with little attention devoted to the problem of response properties. The calculation of static response within Hartree-Fock or Density Functional Theory may be obtained through solution of the Coupled-Perturbed Self-Consistent-Field (CPSCF) equations, which yield properties such as the electric polarizability and hyperpolarizability [7, 8], the Born-effective charge, the nuclear magnetic shielding tensor [9], indirect spin-spin coupling constant [10, 11], geometric derivatives (i.e. higher order analytic force constants) [12] and polarizability derivatives such as the Raman intensity [13, 14], to name but a few.

Conventional approaches to solution of the CPSCF equations [7, 8, 15] are based on perturbation of the wave function, requiring an N^3-scaling eigensolve which may need to be followed by an $\mathcal{O}(N^5)$ transformation of two-electron integrals, depending on the method. In addition to the formal scaling of these conventional methods, they do not admit exploita-

[1]LA-UR-04-5219

tion of quantum locality through the effective use of sparse matrix algebra. More recently, schemes with the potential for reduced complexity have been been put forward. Ochsenfeld and Head-Gordon proposed a scheme based on the Li-Nunes-Vanderbilt density matrix minimization [16]. Later, Larsen *et al.* [17] proposed iterative solution of the CPSCF equations involving equations derived from unitary operations and approximations to the matrix exponential. In both of these approaches, a linear system of equations containing commutation relations is obtained, which *implicitly* determines the response function. However, the method of solution for these equations is not discussed, and computational results are not presented. Recently though, with an apparent reformulation of Ref. [16], Ochsenfeld, Kussmann and Koziol [18] have achieved near linear scaling computation of NMR chemical shifts for one-dimensional alcanes at the GIAO-HF/6-31G* level of theory, but likewise provide no details on their method of solution. These implicit commutation relations are Sylvester-like and may be solved with a number of approaches [19], the particulars of which are of interest.

In contrast, Perturbed Projection [20] is a recently developed alternative for N-scaling solution of the CPSCF equations that is simple and explicit. Based on a recently developed density matrix perturbation theory [21], Perturbed Projection exploits the explicit relationship between the density matrix $\mathcal{D}$ and the effective Hamiltonian or Fockian $\mathcal{F}$ via spectral projection; $\mathcal{D} = \theta(\tilde{\mu}I - \mathcal{F})$, wherein θ is the Heaviside step function (spectral projector) and the chemical potential $\tilde{\mu}$ determines occupied states via Aufbau filling. Spectral projection can be carried out in a number of ways [22–29]. Of special interest here are recursive polynomial expansions of the projector, including the second order trace correcting (TC2) [22] and fourth order trace resetting (TRS4) [23] purification algorithms. These new methods (TC2 and TRS4) have convergence properties that depend only weakly on the band gap, do not require knowledge of the chemical potential and perform well for all occupation to state ratios. Perhaps most important to the current contribution, these methods converge rapidly to smooth, monotone projectors.

Prior to Ref. [18], Perturbed Projection demonstrated linear scaling in computation of the first electric polarizability for three-dimensional water clusters with the Hartree-Fock model

[20]. Also, in a preceding paper, we outlined a non-orthogonal density matrix perturbation theory [30] for response to a change in basis (i.e. as occurs in the evaluation of higher order geometric energy derivatives [12]). In this article, the Perturbed Projection method is extended to higher orders in the electric polarizability, up to fourth order in the total energy.

This paper is organized as follows: First we describe the perturbation expansion and the computation of response properties through solution of the CPSCF equations. Then we present extension of Perturbed Projection through higher orders and the computation of properties using a density matrix analogue of Wigner's $2n + 1$ rule. Next, we present several examples of calculated higher order response properties. We show the saturation of hyperpolarizabilities up to fourth order (i.e. up to the second hyperpolarizability γ) for a series water chains. We also demonstrate linear scaling complexity for the solution of the higher order CPSCF equations and an approximate exponential decay in elements of higher order response functions for 3D water clusters. Finally, we discuss these results and present our conclusions.

II. THE COUPLED PERTURBED SELF-CONSISTENT-FIELD EQUATIONS

The Coupled-Perturbed Self-Consistent-Field (CPSCF) equations yield static response functions and properties in models including both the Hartree-Fock (HF) and Density Functional Theory (DFT). In the following we develop Perturbed Projection for solution of the CPSCF equations in the framework of polarization and Hartree-Fock theory. In many cases, the extension of Perturbed Projection to the computation of other static perturbations is straightforward. In the case of model chemistries that involve DFT, an extra programming effort is required [31, 32]. Also, in the case of properties such as the NMR chemical shift and geometric derivatives (force constants), perturbation of the non-orthogonal basis requires additional considerations that we have detailed in a preceding paper [30].

A Notation

Superscripts and subscripts refer to perturbation order and self-consistent cycle count respectively. The symbols $\mathcal{D}, \mathcal{F}, \ldots$ are matrices in an orthogonal representation, while $D, F, \ldots$ are the corresponding matrices in a non-orthogonal basis. The transformation between orthogonal and non-orthogonal representations is carried out in $\mathcal{O}(N)$ using congruence transformations [33, 34] provided by the approximate inverse (AINV) algorithm for computing sparse approximate inverse Cholesky factors with a computational complexity scaling linearly with the system size [35–37].

B Response expansions

Within HF theory, the total electronic energy E_{tot} of a molecule in a static electric field $\mathcal{E}$ is

$$\begin{aligned} E_{\text{tot}}(\mathcal{E}) &= Tr\{D \cdot (h^0 + \mu\mathcal{E})\} + \frac{1}{2} Tr\{D \cdot (J[D] + K[D])\} \\ &= Tr\{D \cdot F[D]\} - \frac{1}{2} Tr\{D \cdot (J[D] + K[D])\}, \end{aligned} \tag{1}$$

where $D \equiv D[\mathcal{E}]$ is the density matrix in the electric field $\mathcal{E}$, h^0 is the core Hamiltonian, μ is the dipole moment matrix, $J[D]$ is the Coulomb matrix, $K[D]$ the exact HF exchange matrix and

$$F \equiv F[\mathcal{E}] = h^0 + \mu\mathcal{E} + J[D(\mathcal{E})] + K[D(\mathcal{E})] \tag{2}$$

is the Fockian. The total energy of a molecule in a homogeneous electric field may be developed in a Taylor expansion series around $\mathcal{E} = 0$ as

$$\begin{aligned} E_{\text{tot}}(\mathcal{E}) = E_{\text{tot}}(0) &- \sum_a \mu_a \mathcal{E}^a \\ &- \frac{1}{2!} \sum_{ab} \alpha_{ab} \mathcal{E}^a \mathcal{E}^b \\ &- \frac{1}{3!} \sum_{abc} \beta_{abc} \mathcal{E}^a \mathcal{E}^b \mathcal{E}^c \\ &- \frac{1}{4!} \sum_{abcd} \gamma_{abcd} \mathcal{E}^a \mathcal{E}^b \mathcal{E}^c \mathcal{E}^d \\ &+ \dots , \end{aligned} \tag{3}$$

where α_{ab} is the polarizability, and β_{abc} and γ_{abcd} are the first and second hyperpolarizabilities, respectively, μ_a is the dipole moment, and $\mathcal{E}^a$ is the electric field in direction a. The polarizability α_{ab} is the second order response of the total energy with respect to variation in the electric field while the higher derivatives, β_{abc} and γ_{abcd}, give rise to the first and second hyperpolarizabilities [7, 8] where

$$\alpha_{ab} = -\frac{\partial^2 E_{\text{tot}}}{\partial \mathcal{E}^a \partial \mathcal{E}^b}\bigg|_{\mathcal{E}=0} = -2Tr[D^a \mu_b], \tag{4a}$$

$$\beta_{abc} = -\frac{\partial^3 E_{\text{tot}}}{\partial \mathcal{E}^a \partial \mathcal{E}^b \partial \mathcal{E}^c}\bigg|_{\mathcal{E}=0} = -4Tr[D^{ab} \mu_c], \tag{4b}$$

$$\gamma_{abcd} = -\frac{\partial^4 E_{\text{tot}}}{\partial \mathcal{E}^a \partial \mathcal{E}^b \partial \mathcal{E}^c \partial \mathcal{E}^d}\bigg|_{\mathcal{E}=0} = -12Tr[D^{abc} \mu_d]. \tag{4c}$$

Here $D^{a\cdots}$ denotes a density matrix derivative with respect to a field in directions $a\dots$ at $\mathcal{E} = 0$. The density matrix derivative or "response function" is given by

$$\mathcal{D}^{a\cdots} = \frac{\partial^N}{\partial \mathcal{E}^{a\cdots}} \theta(\tilde{\mu} I - \mathcal{F}(\mathcal{E}))\bigg|_{\mathcal{E}=0}. \tag{5}$$

The Fockian may also be expanded order by order in the perturbation to yield

$$\begin{aligned} \mathcal{F}(\mathcal{E}) = \mathcal{F}^0 &+ \sum_a \mathcal{F}^a \mathcal{E}^a \\ &+ \frac{1}{2!} \sum_{ab} \mathcal{F}^{ab} \mathcal{E}^a \mathcal{E}^b \\ &+ \frac{1}{3!} \sum_{abc} \mathcal{F}^{abc} \mathcal{E}^a \mathcal{E}^b \mathcal{E}^c + \dots , \end{aligned} \tag{6}$$

where $\mathcal{F}^a$ stands for $\partial\mathcal{F}(\mathcal{E})/\partial\mathcal{E}^a$, $\mathcal{F}^{ab} = \partial^2\mathcal{F}(\mathcal{E})/\partial\mathcal{E}^a\partial\mathcal{E}^b$, and so on for the higher order terms. A similar expansion also holds for the density matrix $\mathcal{D}(\mathcal{E})$.

Within HF theory, the unperturbed Fockian F^0 in the non-orthogonal basis is

$$F^0 = h^0 + J(D^0) + K(D^0), \tag{7}$$

while the first variation of the Fockian is

$$F^a = \mu_a + J(D^a) + K(D^a) \tag{8}$$

and the higher terms are given by

$$F^{ab\cdots} = J(D^{ab\cdots}) + K(D^{ab\cdots}). \tag{9}$$

In computation of the unperturbed Fockian, the Coulomb matrix J may be computed in $\mathcal{O}(N\lg N)$ with the Quantum Chemical Tree Code (QCTC) [38] and the exchange matrix K computed in $\mathcal{O}(N)$ with the $\mathcal{O}(N)$-exchange (ONX) algorithm that exploits quantum locality of the density matrix D^0 [39]. Likewise the Fockian derivatives, $F^{a\cdots}$, may be computed with the same algorithms in linear scaling time if elements of $D^{a\cdots}$ manifest an approximate exponential decay with atom-atom separation, similar to the decay properties of D^0.

While the expansions above are given explicitly for Hartree-Fock Theory, similar expressions hold also for Kohn-Sham and hybrid HF/DFT, which involve variation of the exchange-correlation matrix $V_{xc}^{a\cdots}(D^0, D^a, \ldots)$ [31, 32].

C Conditions for self-consistency

The derivative density matrices and derivative Fockians depend on each other implicitly, and must be solved for self-consistently via the CPSCF equations. The necessary and sufficient criteria for convergence of the CPSCF equations involve generalized self-consistence

conditions [40],

$$[\mathcal{F}^0, \mathcal{D}^0] = 0, \tag{10}$$

$$[\mathcal{F}^a, \mathcal{D}^0] + [\mathcal{F}^0, \mathcal{D}^a] = 0, \tag{11}$$

$$\begin{aligned}[\mathcal{F}^{ab}, \mathcal{D}^0] + \frac{1}{2}[\mathcal{F}^a, \mathcal{D}^b] + \frac{1}{2}[\mathcal{F}^b, \mathcal{D}^a] \\ + [\mathcal{F}^0, \mathcal{D}^{ab}] = 0,\end{aligned} \tag{12}$$

$$\begin{aligned}[\mathcal{F}^{abc}, \mathcal{D}^0] + \frac{1}{3}[\mathcal{F}^{ab}, \mathcal{D}^c] + \frac{1}{3}[\mathcal{F}^{ac}, \mathcal{D}^b] \\ + \frac{1}{3}[\mathcal{F}^{ab}, \mathcal{D}^c] + \frac{1}{3}[\mathcal{F}^a, \mathcal{D}^{bc}] \\ + \frac{1}{3}[\mathcal{F}^b, \mathcal{D}^{ac}] + \frac{1}{3}[\mathcal{F}^c, \mathcal{D}^{ab}] \\ + [\mathcal{F}^0, \mathcal{D}^{abc}] = 0,\end{aligned} \tag{13}$$

in addition to generalized idempotency-like constraints [40],

$$\mathcal{D}^0 = \mathcal{D}^0\mathcal{D}^0, \tag{14}$$

$$\mathcal{D}^a = \{\mathcal{D}^a, \mathcal{D}^0\}, \tag{15}$$

$$\mathcal{D}^{ab} = \{\mathcal{D}^{ab}, \mathcal{D}^0\} + \frac{1}{2}\{\mathcal{D}^a, \mathcal{D}^b\} \tag{16}$$

$$\begin{aligned}\mathcal{D}^{abc} = \{\mathcal{D}^{abc}, \mathcal{D}_0\} + \frac{1}{3}\{\mathcal{D}^{ab}, \mathcal{D}^c\} + \frac{1}{3}\{\mathcal{D}^{ac}, \mathcal{D}^b\} \\ + \frac{1}{3}\{\mathcal{D}^{bc}, \mathcal{D}^a\},\end{aligned} \tag{17}$$

where the anti-commutator notation $\{A, B\} = AB + BA$ has been used.

III. SOLVING THE HIGHER ORDER CPSCF EQUATIONS WITH PERTURBED PROJECTION

In solution of the CPSCF equations, it is first necessary to determine the ground state density matrix $\mathcal{D}^0$. This may be accomplished in $\mathcal{O}(N)$ using a purification algorithm such as Niklasson's [22] second order trace correcting scheme (TC2) in conjunction with sparse atom-blocked linear algebra [23, 41]. Linear scaling is achieved for insulating systems through the dropping (filtering) of atom-atom blocks with Frobenious norm below a numerical threshold

($\tau \sim 10^{-4} - 10^{-7}$). At SCF convergence the TC2 algorithm generates a polynomial sequence defining the ground state projector, from which the derivative density matrices are directly obtained.

Having solved the groundstate SCF equations, solution of the CPSCF equations commences with a guess at the derivative densities, followed by computation of derivative Fockians. At the r^{th} CPSCF cycle, the n^{th} order derivative Fockians are

$$F_r^{a\cdots} = \begin{cases} \mu_a + J(D_r^a) + K(D_r^a), & n = 1 \\ J(D_r^{a\cdots}) + K(D_r^{a\cdots}), & n > 1\,. \end{cases} \tag{18}$$

After construction of the derivative Fockians, response functions through $D_{r+1}^{a\cdots}$ are computed, constituting one cycle in solution of the CPSCF. As described in Section III A, these response functions are obtained directly through variation of the occupied subspace projector,

$$\mathcal{D}_{r+1}^{a\cdots} = \frac{\partial^n}{\partial \mathcal{E}^{a\cdots}} \theta(\tilde{\mu} I - \mathcal{F}_r(\mathcal{E}))\Big|_{\mathcal{E}=0}, \tag{19}$$

which is accomplished via the Niklasson and Challacombe density matrix perturbation theory [21].

After a few CPSCF cycles, the approach to self-consistency may be accelerated with Weber and Daul's DDIIS algorithm [42],

$$\widetilde{\mathcal{F}}_r^{a\cdots} = \sum_{k=r-s}^{r} c_k \mathcal{F}_k^{a\cdots} \tag{20}$$

in which the c_k coefficients are chosen to minimize the n^{th} order commutation relations, as in Eqs. (11)-(13). The application of the DDIIS algorithm to acceleration of higher order CPSCF equations is developed further in Section III B.

At self-consistency, the conditions given in Section II C have been met, and it is then appropriate to compute response properties. In general, we can use the expectation value

$$E^{(\gamma)} = 2(\gamma - 1)! Tr(D^{(\gamma-1)} h^{(1)}), \tag{21}$$

where in the case of polarization we have the (hyper)polarizabilities $\alpha_{ab} = -2\text{Tr}[D^a \mu_b]$, $\beta_{abc} = -4\text{Tr}[D^{ab} \mu_c]$ or $\gamma_{abcd} = -12\text{Tr}[D^{abc} \mu_d]$. Alternatively, it is possible to construct

density matrix analogues of Wigner's $2n+1$ rule, which allows the evaluation of response properties up to order $2n+1$ from response functions of order n. These analogues are given in Section III C through 4^{th} order in the energy.

A Perturbed Projection

Although a number of analytic, asymptotically discontinuous representations exist for the Heaviside step function θ, direct representation (and variation) of these forms as in Eq. (19) is problematic. Polynomial expansion of the step function is a alternative choice, but demands a very high order and can be costly. Specifically, polynomial expansion of θ with a p'th order polynomial incurs a cost that is at best $\mathcal{O}(\sqrt{p})$ [43]. Polynomial expansion techniques, such as those based on the the Tchebychev polynomials, may also be plagued by Gibbs oscillations [44], which are high order ripples in the approximate θ due to incompleteness. Alternatively, recursive purification methods achieve high order representation in $\mathcal{O}(\log p)$ [23]. Also, purification methods (such as TC2 and TRS4) yield projectors that are smooth and strictly monotonic,

Each Perturbed Projection sequence is based on a corresponding purification scheme or generator, such as TC2 [22]. The Perturbed Projection sequence is obtained by collecting terms of the response order by order upon perturbative expansion of its generator [21]. Perturbed Projection provides explicit, recursive formulae for the construction of response functions, retaining the convergence properties, smoothness and montonicity of the generating sequence. These explicit formulae stand in contrast to methods where the density matrix derivatives are implicitly defined as solutions to equations of Sylvester type [16–18].

Sufficient to compute fourth order properties using the $2n+1$ rule presented in Section III C, Perturbed Projection is outlined in the following for computation of the second order response function. The Perturbed Projection sequence is started with the $\mathcal{X}_0^{a\cdots}$, which are prepared from the Fockians $\mathcal{F}^0$, $\mathcal{F}^a$, and $\mathcal{F}^{ab}$ by compressing their spectrum into the domain

of convergence [22] using

$$\mathcal{X}_0^0 = \frac{\mathcal{F}_{max} - \mathcal{F}^0}{\mathcal{F}_{max} - \mathcal{F}_{min}} \tag{22}$$

and

$$\mathcal{X}_0^{a\cdots} = \frac{\mathcal{F}_n^{a\cdots}}{\mathcal{F}_{min} - \mathcal{F}_{max}}, \tag{23}$$

where $\mathcal{F}_{min}$ and $\mathcal{F}_{max}$ are upper and lower bounds to the eigenvalues of $\mathcal{F}^0$.

While Perturbed Projection can be formulated within any purification scheme, we focus here on the simple and efficient TC2 method [22]. Briefly, TC2 constructs a ground state projector through a series of trace correcting projections; when the trace is larger than N_e, x^2 is used to reduce the trace, and when the trace is less than N_e, $2x - x^2$ is used to increase the trace. The resulting sequence of correcting projections yields a step at the correct chemical potential. Within this framework, the second order TC2 Perturbed Projection sequence is

$$\left.\begin{aligned} \mathcal{X}_{i+1}^{ab} &= \{\mathcal{X}_i^{ab}, \mathcal{X}_i^0\} + \tfrac{1}{2}\{\mathcal{X}_i^a, \mathcal{X}_i^b\} \\ \mathcal{X}_{i+1}^{a} &= \{\mathcal{X}_i^{a}, \mathcal{X}_i^0\} \\ \mathcal{X}_{i+1}^{b} &= \{\mathcal{X}_i^{b}, \mathcal{X}_i^0\} \\ \mathcal{X}_{i+1}^{0} &= (\mathcal{X}_i^0)^2 \end{aligned}\right\} \mathrm{Tr}[\mathcal{X}_i^0] \geq N_e \tag{24}$$

or

$$\left.\begin{aligned} \mathcal{X}_{i+1}^{ab} &= 2\mathcal{X}_i^{ab} - (\{\mathcal{X}_i^{ab}, \mathcal{X}_i^0\} + \tfrac{1}{2}\{\mathcal{X}_i^a, \mathcal{X}_i^b\}) \\ \mathcal{X}_{i+1}^{b} &= 2\mathcal{X}_i^{b} - \{\mathcal{X}_i^{b}, \mathcal{X}_i^0\} \\ \mathcal{X}_{i+1}^{a} &= 2\mathcal{X}_i^{a} - \{\mathcal{X}_i^{a}, \mathcal{X}_i^0\} \\ \mathcal{X}_{i+1}^{0} &= 2\mathcal{X}_i^{0} - (\mathcal{X}_i^0)^2 \end{aligned}\right\} \mathrm{Tr}[\mathcal{X}_i^0] < N_e. \tag{25}$$

As with the TC2 generator, the n^{th} order response functions

$$\mathcal{D}^{a\cdots} = n! \lim_{i\to\infty} \mathcal{X}_i^{a\cdots}, \tag{26}$$

converge quadratically, reaching convergence when either the error $\varepsilon = |\mathrm{Tr}[\mathcal{X}_i^0] - N_e| + |\mathrm{Tr}[\mathcal{X}_i^a]| + \ldots$, or the maximum element in the change $\delta\mathcal{X}^{a\cdots} = |\mathcal{X}_{i+1}^{a\cdots} - \mathcal{X}_i^{a\cdots}|$ falls below τ, the atom-atom block drop tolerance described in Ref. [23]. As described more completely in Ref. [30], when the solution gets close to convergence, i.e. $|\mathrm{Tr}[\mathcal{X}_i^0] - N_e| < \epsilon$ with $\epsilon \approx$

$10^{-1} - 10^{-3}$, we alternate the projection at each step, which protects the convergence under the incomplete sparse linear algebra.

B Derivative DIIS

Direct inversion in the iterative subspace (DIIS), introduced some time ago by Pulay [45, 46], accelerates convergence toward self-consistency. DIIS employs information accumulated during preceding iterations to construct an effective Fockian $\widetilde{\mathcal{F}}_k$ at the k-th SCF cycle, which minimizes the commutation error between the Fockian and the density matrix. The effective Fockian is then used instead of $\mathcal{F}_k$ to generate an improved density matrix.

Recently, Weber and Daul have developed the Derivative DIIS (DDIIS) scheme for accelerating convergence of the CPSCF equations [42]. Like DIIS, DDIIS is based on minimization of the Frobenious norm of an error matrix

$$\widetilde{e}_r^{a\cdots} = \sum_{i=r-s}^{r} c_i e_i^{a\cdots}, \tag{27}$$

where the $e_i^{a\cdots}$'s are just the n-th order commutator relation of Eqs. (10-13) (e.g. the first order error matrix is given by $e_i^a = [\mathcal{F}_i^a, \mathcal{D}^0] + [\mathcal{F}^0, \mathcal{D}_i^a]$). The optimal coefficients c_i are solutions to the quadratic programming problem

$$\inf\left\{ -\frac{1}{2} \sum_{i,j=r-s}^{n} c_i B_{ij} c_j,\ \sum_{i=r-s}^{r} c_i = 1 \right\}, \tag{28}$$

where elements of the $\mathbf{B}$ matrix are given by $B_{ij} = \mathrm{Tr}[e_i^{a\cdots}(e_j^{a\cdots})^T]$. A working equation is then obtained through the associated Euler-Lagrange equation

$$\begin{pmatrix} \mathbf{B} & \mathbf{1} \\ \mathbf{1}^T & 0 \end{pmatrix} \cdot \begin{pmatrix} \mathbf{c} \\ \lambda \end{pmatrix} = \begin{pmatrix} \mathbf{0} \\ 1 \end{pmatrix}, \tag{29}$$

where $\mathbf{0} = (0, \ldots, 0)^T$ and $\mathbf{1} = (1, \ldots, 1)^T$ are vectors whose components are 0 and 1 respectively and λ is the Lagrange multiplier of the constraint $\sum_{i=n-m}^{n} c_i = 1$. The set of linear equations is solved by inverting the left-hand side matrix. In the event of a singular or near singular matrix, the rank of Eq. (29) is reduced by discarding the oldest entries (increasing s) until the linear system stabilizes.

C Density matrix formulation of Wigner's $2n+1$ rule

Wigner's $2n+1$ rule, traditionally predicated on derivatives of the wavefunction, yields order $2n+1$ in the energy response from n-th order derivatives [8, 47]. A density matrix analogue of Wigner's $2n+1$ rule for a single perturbation parameter was given to third order by McWeeny [48] and up to fourth order by Niklasson and Challacombe [21] in the orthogonal representation. For completeness, we present non-orthogonal generalizations up to fourth order, which may require less memory due to the less dense structure of non-orthogonal matrix intermediates.

The first and second order energy corrections are well known, corresponding simply to expectation values as in Eq. (21). Beyond second order, the $2n+1$ rule offers a valuable alternative. The third order non-orthogonal contribution is

$$E^{abc} = 2 \sum_{P(a,b,c)} \mathrm{Tr}[[D^a, D^0]_S S D^b F^c] \tag{30}$$

where $P(a,b,c)$ stands for the permutation operator such that all permutations of a, b and c are made (e.g. $P(a,b,c)$ generates the sum of all the six terms: (a,b,c), (a,c,b), (b,a,c), (b,c,a), (c,a,b) and (c,b,a)) and $[A,B]_S = ASB - BSA$ where S is the overlap matrix. Similarly, the fourth order non-orthogonal contribution is

$$\begin{aligned} E^{abcd} = \sum_{P(a,b,c,d)} \mathrm{Tr}[[D^{ab}, D^0]_S S D^c F^d + \\ [D^a, D^0]_S S (D^{bc} F^d + D^b F^{cd})] \end{aligned} \tag{31}$$

For the orthogonal case $S = I$ and $D^a, F^c, \ldots$ are replaced by $\mathcal{D}^a, \mathcal{F}^c, \ldots$. In most cases the complexity of these equations can be reduced by taking advantage of indicial symmetry; a, b, c, and d represent the Cartesian directions x, y, z so that terms with indecies in the same direction simplify. For example, E^{aaaa} reduces to only one term requiring only 15 matrix multiplications. In the worst case, where all the directions are different, i.e. E^{aabc} (or any other permutation of (a,a,b,c)), the relation (31) reduces to include only 12 terms with 180 matrix multiplications. Similar reductions of the computational cost also apply to

Eq. (30). The number of matrix-matrix multiplies can be further reduced if one uses an orthogonal representation, but this typically involves matrix-matrix multiplies with more dense intermediates.

IV. RESULTS

We have implemented these methods in the MondoSCF suite of linear scaling quantum chemistry programs [50]. The construction of the Fockian and derivative Fockian was carried out using the linear scaling QCTC method for computation of the Coulomb matrix [38, 51] and the ONX algorithm [39, 52] for computation of the Hartree-Fock exchange matrix. The CPSCF equations were solved in an entirely orthogonal representation, with higher order properties evaluated using the $2n + 1$ rule with the non-orthogonal formulae given by Eqs. (30-31). Two different levels of numerical accuracy have been used, `GOOD` and `TIGHT`. Thresholds that define the `GOOD` accuracy level include a matrix threshold $\tau = 10^{-5}$, as well as other numerical thresholds detailed in Ref. [51], which deliver 6 digits of relative accuracy in the total energy. The `TIGHT` option involves the matrix threshold $\tau = 10^{-6}$ and delivers 8 digits of relative accuracy in the total energy.

Calculations were carried out on a single Intel Xeon 2.4GHz processor running RedHat Linux 8.0 and executables compiled with Portland Group Fortran Compiler pgf90 4.0-2 [53].

Convergence of the CPSCF equations for the water systems described in the following are typically achieved in about 10 cycles, independent of cluster size, basis set, matrix threshold or order of the response calculated.

All results are reported in atomic units. Also, unless otherwise noted, all timings and values have been obtained by computing the n^{th} order response function and evaluation with the $n + 1$ rule (expectation value), Eq. (21).

A One dimensional water chains

Perturbed Projection has been used to compute the (hyper)polarizabilities α_{zz}, β_{zzz} and γ_{zzzz} of linear water chains up to $(H_2O)_{20}$. These calculations have been carried out with MondoSCF at the RHF/6-31G level of theory using both the `GOOD` and `TIGHT` thresholding parameters, as well as with the conventional algorithms implemented in the GAMESS quantum chemistry package [49]. These static properties have been evaluated at the geometries given by Otto *et al.* [54], and the GAMESS results are given to the number of digits provided by that program. The MondoSCF results have been obtained both as expectation values, given by Eq. (21), and using the non-orthogonal density matrix $2n + 1$ rules given in Eqs. (30-31).

As a benchmark, we have also carried out calculations with the linear chain $(H_2O)_{20}$ with the `VERYTIGHT` numerical thresholding parameters, which employ a 10^{-7} drop tolerance and aim to provide 10 digits of precision in the total energy. These `VERYTIGHT` calculations yield $\alpha_{zz} = 7.142422\,a.u.$, $\beta_{zzz} = -12.033362\,a.u.$ and $\gamma_{zzzz} = 1411.425500\,a.u.$.

B Linear scaling: 3D water clusters

Linear scaling computation of the RHF/6-31G and RHF/6-31G** second hyperpolarizability, achieved with Perturbed Projection, is shown for three-dimensional water clusters in Fig 1. These timings are the total CPU time for the fifth CPSCF cycle, including build time for $\mathcal{F}^{abc}$ (ONX and QCTC), iterative construction of $\mathcal{D}^{abc}$ (Perturbed Projection via TC2) and all intermediate steps including the congruence transformation. A breakdown of the dominant contributions to these totals are given in Figs 2-4, which show timings for Coulomb summation (QCTC), Perturbed Projection (TC2), and exact exchange (ONX).

Figure 5 shows the increase in cost associated with computing higher order response functions. Corresponding to this increase in cost, Fig. 6 shows the magnitude of atom-atom blocks of density matrix derivatives up to third order as a function of atom-atom distance

when perturbed by a static electric field. The density response shows an approximate exponential decay as a function of internuclear distance with the rate of decay slowing slightly and the distribution shifted up with increasing order in the perturbation.

V. DISCUSSION

In our current formulation, the increase in magnitude and reduction of locality in elements of the response function makes achieving linear scaling more difficult with increasing order in perturbation. Nevertheless, linear scaling has been achieved at the HF level of theory up to fourth order (i.e. γ) in the total energy for three-dimensional systems and non-trivial basis sets. At fourth order, Perturbed Projection and exact exchange were the dominant costs in solving the CPSCF equations, as shown in Figs 3 and 4. For the fourth order Perturbed Projection, N-scaling is achieved between 70 to 110 water molecules, depending on τ. Despite a nearly dense D^{abc}, the dominant work in its construction always involves multiplication with matrices that are significantly more sparse, as $\mathcal{X}_i^{abc}\mathcal{X}_i^0$ or $\mathcal{X}_i^{ab}\mathcal{X}_i^c$. Likewise, N-scaling is achieved between 70 to 90 water molecules for construction of the Hartree-Fock exchange contribution. In this case, the approximate decay of the density matrix still leads to linear scaling through ordered skip out lists, as described in Ref. [39]. In both cases, the increase in response function magnitude is equivalent to tightening numerical thresholds, which increases the cost and delays the onset of linear scaling.

In tables I-III we find that a reduction of the drop tolerance by one order of magnitude leads to an increase in precision by 1-2 significant digits, with `GOOD` and `TIGHT` yielding approximatively 3-4 and 5-6 correct digits independent of the response order. We further observe about 1 extra digit of accuracy when using the $2n+1$ rule. This might be expected from the higher order error propagation resulting from products of lower order response functions, relative to evaluation with Eq. (21), which involves an error that is always linear in a higher order derivative density matrix.

As shown in Fig. 5, computing the second order response is significantly cheaper than the

third order response, and involves an earlier onset of linear scaling. Because evaluation of properties with the $2n+1$ rule is of negligible cost relative to solving the CPSCF equations, the cost difference for evaluating γ with the $2n+1$ rule relative to the $n+1$ expectation is just the difference (roughly 2:3) between the computation of β and γ shown in Fig. 5.

VI. CONCLUSIONS

Linear scaling has been demonstrated for the computation of response properties beyond second order in the total energy using Perturbed Projection for solution of the Coupled-Perturbed Self-Consistent-Field equations. In addition, we have provided details of the computational method, used three-dimensional systems and non-trivial basis sets to demonstrate linear scaling and provided a (preliminary) assessment of error control. Perturbed Projection for the computation of higher order response functions is quadratically convergent, simple to implement through higher orders and numerically stable. Perturbed Projection is not unique to the Hartree-Fock model, the TC2 generator or the MondoSCF N-scaling algorithms, but can be straightforwardly extended to models that include exchange correlation (DFT), other other purification schemes such as TRS4 [23] as well as other electronic structure programs.

We have shown that response functions (density matrix derivatives) through fourth order are local upon *global* electric perturbation, corresponding to an approximate exponential decay of matrix elements. However, the magnitude of the corresponding response functions increases with increasing perturbation order, equivalent to tightening of the matrix drop tolerance, τ. While we have not attempted to work out a detailed analysis for the propagation of error, it may be possible to develop a more effective thresholding scheme for high orders. In addition to being somewhat more accurate, the $2n+1$ rule also provides a significantly cheaper alternative to the computation of expectation values and an earlier onset of linear scaling.

A similar exponential decay in the first order response corresponding to a *local* nuclear

displacement has likewise been demonstrated by Ochsenfeld and Head-Gordon [16]. This behavior is expected to hold generally for both local and global perturbations to insulating systems. Thus, the potential exists for Perturbed Projection to achieve linear scaling for a large class of static molecular properties within the HF, DFT and hybrid HF/DFT model chemistries. Of particular interest, the recently developed non-orthogonal density matrix perturbation theory put forward in a proceeding article [30] may enable linear scaling computation of analytic second derivatives, which are important in computation of the Hessian matrix.

ACKNOWLEDGMENTS

This work has been supported by the US Department of Energy under contract W-7405-ENG-36 and the ASCI project. The Advanced Computing Laboratory of Los Alamos National Laboratory is acknowledged. All the numerical computations have been performed on computing resources located at this facility.

REFERENCES

† Electronic address: valery.weber@unifr.ch

[1] G. Galli, Cur. Op. Sol. State Mat. Sci. **1**(6), 864 (1996).

[2] D. R. Bowler, M. Aoki, C. M. Goringe, A. P. Horsfield, and D. G. Pettifor, Mod. Sim. Mat. Sci. Eng. **5**(3), 199 (1997).

[3] S. Goedecker, Rev. Mod. Phys. **71**, 1085 (1999).

[4] P. Ordejon, Phys. Status Solidi B **217**(1), 335 (2000).

[5] V. Gogonea, D. Suarez, A. van der Vaart, and K. W. Merz, Curr. Opin. Struct. Biol. **11**(2), 217 (2001).

[6] S. Y. Wu and C. S. Jayanthi, Phys. Rep. **358**, 1 (2002).

[7] H. Sekino and R. J. Bartlett, J. Chem. Phys. **85**, 976 (1986).

[8] S. P. Karna and M. Dupuis, J. Comput. Chem. **12**, 487 (1991).

[9] K. Wolinski, J. F. Hinton, and P. Pulay, jacs **112**, 8251 (1990).

[10] C. H. Pennington and C. P. Slichter, Phys. Rev. Lett. **66**, 381 (1991).

[11] O. L. Malkina, D. R. Salahub, and V. G. Malkin, J. Chem. Phys. **105**, 8793 (1996).

[12] R. Amos and J. E. Rice, Comp. Phys. Rep. **10**, 147 (1989).

[13] M. Lazzeri and F. Mauri, Phys. Rev. Lett. **90**, 36401 (2003).

[14] O. Quinet and B. Champagne, J. Chem. Phys. **115**, 6293 (2001).

[15] J. Pople, R. Krishnan, H. B. Schlegel, and J. S. Binkley, ijqcs **S13**, 225 (1979).

[16] C. Ochsenfeld and M. Head-Gordon, Chem. Phys. Lett. **270**, 399 (1997).

[17] H. Larsen, T. Helgaker, J. Olsen, and P. Jorgensen, J. Chem. Phys. **115**, 10344 (2001).

[18] C. Ochsenfeld, J. Kussmann, and F. Koziol, Angewandte Chemie **43**, 4485 (2004).

[19] J. Brandts, Lect. Notes Comp. Sci **2179**, 462 (2001).

[20] V. Weber, A. M. N. Niklasson, and M. Challacombe, Phys. Rev. Lett. **92**, 193002 (2004).

[21] A. M. N. Niklasson and M. Challacombe, Phys. Rev. Lett. **92**, 193001 (2004).

[22] A. M. N. Niklasson, Phys. Rev. B **66**, 155115 (2002).

[23] A. M. N. Niklasson, C. J. Tymczak, and M. Challacombe, J. Chem. Phys. **118**(19), 8611 (2003).

[24] R. McWeeny, Rev. Mod. Phys. **32**, 335 (1960).

[25] W. L. Clinton, A. J. Galli, and L. J. Massa, Phys. Rev. **177**(1), 7 (1969).

[26] A. H. R. Palser and D. E. Manolopoulos, Phys. Rev. B **58**, 12704 (1998).

[27] G. Beylkin, N. Coult, and M. J. Mohlenkamp, J. Comp. Phys. **152**(1), 32 (1999).

[28] K. Nemeth and G. E. Scuseria, J. Chem. Phys. **113**(15), 6035 (2000).

[29] A. Holas, Chem. Phys. Lett. **340**(5–6), 552 (2001).

[30] A. M. N. Niklasson, V. Weber, and M. Challacombe, *Density matrix perturbation theory for non-orthogonal representations* (2005), submitted to the Journal of Chemical Physics.

[31] A. M. Lee and S. M. Colwell, J. Chem. Phys. **101**, 9704 (1994).

[32] P. Salek, O. Vahtras, T. Helgaker, and H. Ågren, J. Chem. Phys. **117**, 9630 (2002).

[33] J. H. Wilkinson, *The aglebraic Eigenvalue Problem* (Clarendon Press, Oxford, 1965).

[34] G. W. Stewart, *Introduction to Matrix Computations* (Acadmeic Press, London, 1973).

[35] M. Benzi and C. D. Meyer, SIAM J. Sci. Comput. **16**(5), 1159 (1995).

[36] M. Benzi, C. D. Meyer, and M. Tůma, SIAM J. Sci. Comput. **17**(5), 1135 (1996).

[37] M. Benzi, R. K. R, and M. Tuma, Comp. Meth. App. Mech. Eng. **190**(49-50), 6533 (2001).

[38] M. Challacombe and E. Schwegler, J. Chem. Phys. **106**, 5526 (1997).

[39] E. Schwegler, M. Challacombe, and M. Head-Gordon, J. Chem. Phys. **106**, 9708 (1997).

[40] F. Furche, J. Chem. Phys. **114**, 5982 (2001).

[41] M. Challacombe, Comput. Phys. Commun. **128**, 93 (2000).

[42] V. Weber and C. Daul, Chem. Phys. Lett. **370**, 99 (2003).

[43] W. Z. Liang, R. Baer, C. Saravanan, Y. H. Shao, A. T. Bell, and M. Head-Gordon, J. Comp. Phys. **194**, 575 (2004).

[44] A. F. Voter, J. D. Kress, and R. N. Silver, Phys. Rev. B **53**, 12733 (1996).

[45] P. Pulay, Chem. Phys. Let. **73**(2), 393 (1980).

[46] P. Pulay, J. Comput. Chem. **3**(4), 556 (1982).

[47] S. T. Epstein, *The Variation Method in Quantum Chemistry* (Academic Press, San Fransisco, 1974).

[48] R. McWeeny, Rev. Mod. Phys. **126**, 1028 (1962).

[49] M. W. Schmidt, K. K. Baldridge, J. A. Boatz, S. T. Elbert, M. S. Gordon, J. H. Jensen, S. Koseki, N. Matsunaga, K. A. Nguyen, S. Su, T. L. Windus, M. Dupuis, *et al.*, J. Comp. Chem. **14**, 1347 (1993).

[50] M. Challacombe, E. Schwegler, C. J. Tymczak, C. K. Gan, K. Nemeth, V. Weber, A. M. N. Niklasson, and G. Henkelman, MondoSCF *v1.0α9, A program suite for massively parallel, linear scaling SCF theory and ab initio molecular dynamics.* (2001), URL `http://www.t12.lanl.gov/home/mchalla/`, Los Alamos National Laboratory (LA-CC 01-2), Copyright University of California.

[51] C. J. Tymczak and M. Challacombe, *Linear scaling computation of the Fock matrix. VIII. Periodic Density Functional Theory at the* Γ*-point* (2004), cond-mat/0405500, To appear

in J. Chem. Phys.

[52] C. J. Tymczak, V. Weber, E. Schwegler, and M. Challacombe, *Linear scaling computation of the Fock matrix. IX. Periodic boundaries for exact exchange at the* Γ*-point* (2004), cond-mat/0406094, To appear in J. Chem. Phys.

[53] The Portland Group, *pgf90 v4.2* (2002), URL `http://www.pgroup.com/`.

[54] P. Otto, F. L. Gu, and J. Ladik, J. Chem. Phys. **110**, 2717 (1999).

TABLES

TABLE I: The longitudinal polarizability, α_{zz}, for water chains at the RHF/6-31G level of theory, computed with MondoSCF using `GOOD` and `TIGHT` numerical thresholds, and also with the GAMESS quantum chemistry package [49].

N_{H_2O}	GAMESS	`GOOD`	`TIGHT`
1	5.8136	5.813620	5.813588
2	6.3448	6.345037	6.344822
3	6.5844	6.584658	6.584435
4	6.7276	6.727905	6.727672
5	6.8226	6.823290	6.822857
10	7.0308	7.031056	7.030858
15	7.1047	7.104904	7.104770
20	7.1424	7.142580	7.142422

TABLE II: The longitudinal first hyperpolarizability, β_{zzz}, for water chains at the RHF/6-31G level of theory, computed with MondoSCF using `GOOD` and `TIGHT` numerical thresholds, and also with the GAMESS quantum chemistry package [49].

N_{H_2O}	GAMESS	`GOOD`	`GOOD`[a]	`TIGHT`	`TIGHT`[a]
1	-30.6125	-30.611029	-30.612627	-30.612163	-30.612256
2	-29.5444	-29.547427	-29.548504	-29.544907	-29.544994
3	-25.3696	-25.372208	-25.373615	-25.370297	-25.370381
4	-22.1411	-22.143436	-22.145040	-22.141494	-22.141603
5	-19.8925	-19.902088	-19.904449	-19.896462	-19.897141
10	-14.8063	-14.807075	-29.617990	-14.806973	-14.807119
15	-12.9713	-12.969238	-12.972227	-12.971940	-12.972124
20	-12.0334	-12.028709	-12.033633	-12.034014	-12.034238

[a]The density matrix based 2n+1 rule has been used.

TABLE III: The longitudinal second hyperpolarizability, γ_{zzzz}, for water chains at the RHF/6-31G level of theory, computed with MondoSCF using `GOOD` and `TIGHT` numerical thresholds, and also with the GAMESS quantum chemistry package [49].

N_{H_2O}	GAMESS	`GOOD`	`GOOD`[a]	`TIGHT`	`TIGHT`[a]
1	330.5753	330.54375	330.54319	330.57193	330.5724
2	820.1398	820.19231	820.19667	820.14775	820.1493
3	1008.5656	1008.5855	1008.6073	1008.5752	1008.5765
4	1103.4813	1103.5053	1103.5280	1103.4883	1103.4902
5	1168.9563	1169.2104	1169.2531	1169.0630	1169.0754
10	1324.2906	1325.1208	1324.6321	1324.2975	1324.2999
15	1381.8657	1383.0802	1382.2322	1381.8758	1381.8738
20	1411.4264	1414.4092	1411.8528	1411.4410	1411.4292

[a]The density matrix based 2n+1 rule has been used.

FIGURES

FIG. 1: Total CPU time of the fifth CPSCF iteration of fourth order for the water cluster sequence with the 6-31G and 6-31G** basis sets and the `GOOD` and `TIGHT` numerical thresholds (see text) controlling numerical precision of the result. The lines are fits to the last three and four points, respectively.

FIG. 2: QCTC CPU time of the fifth CPSCF iteration of fourth order for the water cluster sequence with the 6-31G and 6-31G** basis sets and the `GOOD` and `TIGHT` numerical thresholds (see text) controlling numerical precision of the result. The lines are fits to the last three and four points, respectively.

FIG. 3: TC2 CPU time of the fifth CPSCF iteration of fourth order for the water cluster sequence with the 6-31G and 6-31G** basis sets and the `GOOD` and `TIGHT` numerical thresholds (see text) controlling numerical precision of the result. The lines are fits to the last three and four points, respectively.

FIG. 4: ONX CPU time of the fifth CPSCF iteration of fourth order for the water cluster sequence with the 6-31G and 6-31G** basis sets and the `GOOD` and `TIGHT` numerical thresholds (see text) controlling numerical precision of the result. The lines are fits to the last three and four points, respectively.

FIG. 5: Total CPU times with increasing order of the response for the fifth CPSCF cycle computed as the $n+1$ expectation value, Eq. (21).

FIG. 6: Superposition of the magnitudes of the RHF/6-31G density matrix derivative elements D_{cd}, D^{x}_{cd}, D^{xx}_{cd} and D^{xxx}_{cd} along the x axis with the separation of basis function centers for $(H_2O)_{150}$. The density matrix derivatives have been converged to within `TIGHT` (e.g. a matrix threshold $\tau = 10^{-6}$ $[a.u.]$).

Figure 1, V. Weber, A. Niklasson, and M. Challacombe

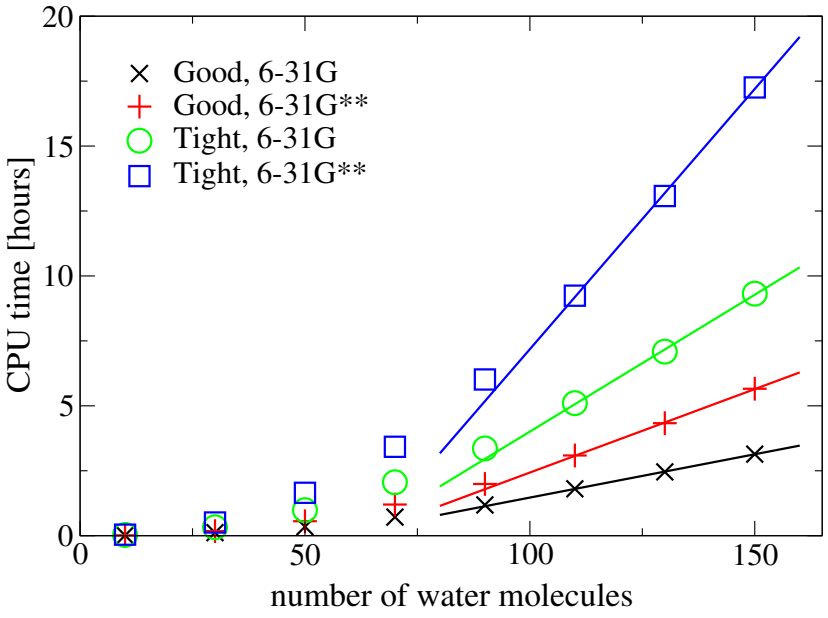

Figure 2, V. Weber, A. Niklasson, and M. Challacombe

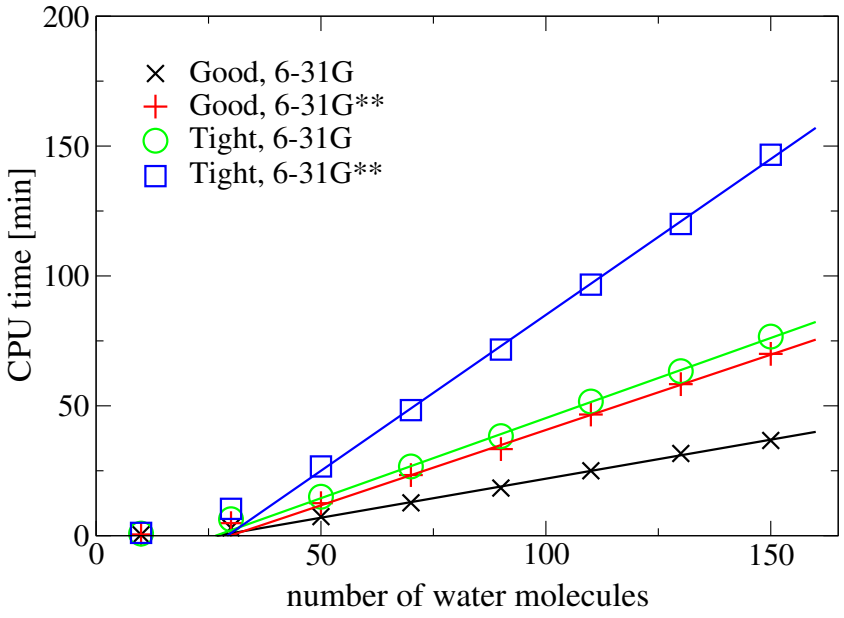

Figure 3, V. Weber, A. Niklasson, and M. Challacombe

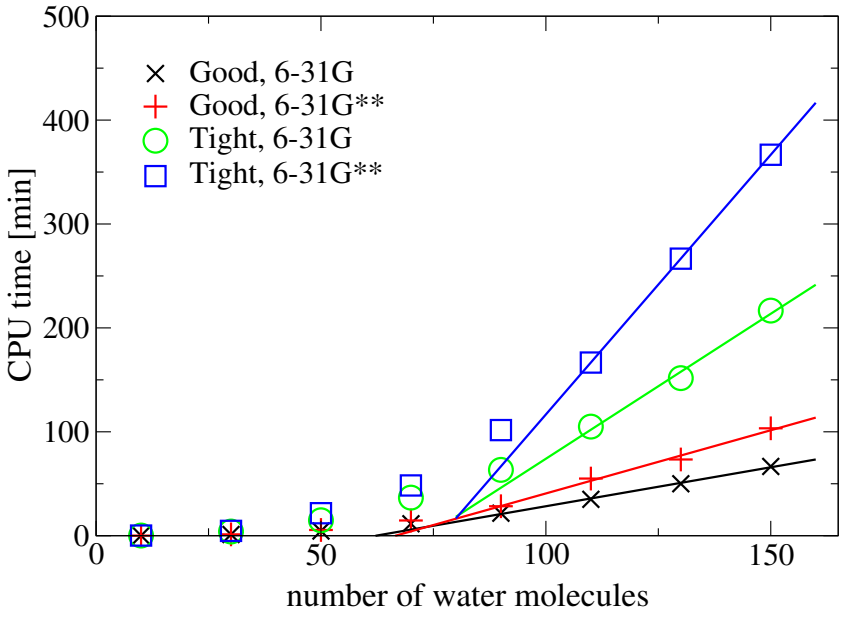

Figure 4, V. Weber, A. Niklasson, and M. Challacombe

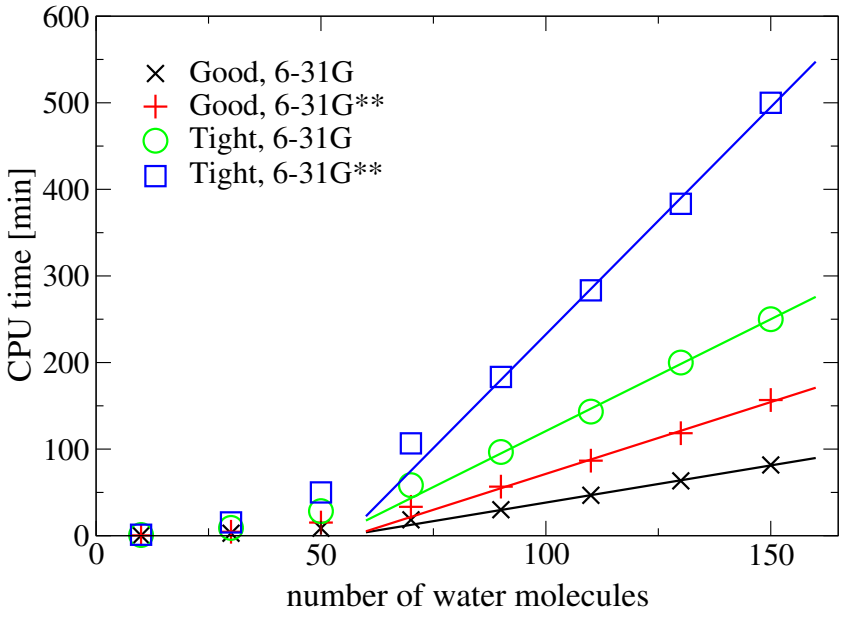

Figure 5, V. Weber, A. Niklasson, and M. Challacombe

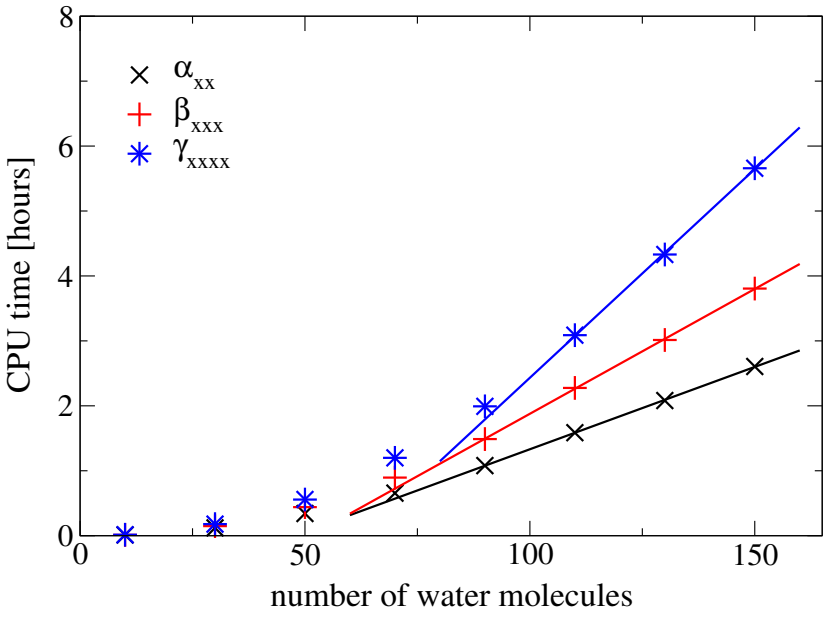

Figure 6, V. Weber, A. Niklasson, and M. Challacombe